Publ. Astron. Obs. Belgrade No. 76 (2003), 85-104 *Invited lecture*

DIAGNOSTICS OF MAGNETOPLASMA COMPRESSOR OF COMPACT GEOMETRY

J. PURIĆ[1,2], I.P. DOJČINOVIĆ[1] , V.M. ASTASHYNSKI[3], M.M. KURAICA[1,2]

[1] *Faculty of Physics, University of Belgrade, P.O. Box 368, 11001 Belgrade, Serbia*

[2] *Center for Science and Technology Development, Obilicev Venac 26, Belgrade, Serbia*

[3] *Institute of Molecular and Atomic Physics, National Academy of Sciences of Belarus, F. Skaryna Avenue 70, 220072 Minsk, Belarus*

Abstract. Quasistationary plasma accelerator of magnetoplasma compressor type with semitransparent electrodes operating in an ion current transfer regime has been constructed and studied. Main discharge and compression plasma flow parameters have been measured. It has been found that the current cut off limiting the increase of the parameters in the case of classical plasma accelerators operating in the electron current transfer can be avoided by switching to the ion current transfer. It was made achievable by an especially designed electrode system shielded by the magnetic field, and therefore protected of the erosion as a main reason for energy losses leading to the current crisis. Due to the electrode transparency in two stage quasistationary plasma accelerator there is no limit in the maximal current value depending only on the condenser bank input energy used in the experiment. Consequently, the compression plasma flow velocity, electron density and temperature depend only on the energy transfer efficiency from supply source to plasma. It has been concluded that the efficiency is maximal when operating in the hydrogen in comparison with other working gases (argon, nitrogen etc.). It was found that, for an input energy of 6.4 kJ the maximal values of plasma flow velocity and electron density are of the order of ~100 km/s and ~10^{17} cm^{-3}, respectively. These accelerating systems are of special interest for development of new plasma technologies such as plasma solid surface modification and obtaining new materials including nano sized ones. Finally, these accelerators can be used for construction of plasma injectors to fusion devices.

1. INTRODUCTION

Traditional plasma accelerators have achieved a certain limit in their development and application (Morozov, 1990). The potential of farther increase of their plasma parameters practically has been exhausted in such accelerators (with inherent magnetic field and electron current transfer). Namely, in order to increase the plasma parameters, the discharge current of accelerator has to be increased. However, the increase in discharge current causes intense potential jump near the electrode (anode or cathode) and its heavy erosion (Morozov, 1969). There is no way to overcome this phenomenon within the concept of electron current transfer. That is why transition to systems with an ion current transfer is necessary (Morozov, 1990). Such systems are the quasistationary plasma accelerators of new generation. The plasma acceleration in a discharge device of these

accelerators is accompanied by compression flow formation at the outlet with plasma parameters much higher than those in inter-electrode gap. These accelerator systems are of special interest for development of new plasma technologies. High plasma parameters of compression flows, together with large discharge duration enable efficient usage of such flows for material surface modification. The duration of compression plasma flow in different material processing is very important, particularly for solid surface modifications and the investigation of plasma wall interaction, important for fusion research.

Magnetoplasma compressor (MPC) is the source of quasistationary compression plasma flows (Morozov, 1975). The importance of research connected with the MPC and the creation of compression plasma flows is not only in enabling the study of fundamental processes in plasma flows and their behavior in different configurations of electric and magnetic fields, but also, in application of such systems and their plasma flows in different plasma technologies. For example, they are very intensive radiation source from X-ray to microwave region. Also, they can be used for the hardening of different materials (such as steal and its alloys, for instance) surfaces, plasma deposition of the materials on the sample surfaces and its modifications including creation of submicrostructures of silicon and other semiconductors (Astashynski *et al*., 2002ab); acceleration of micro particles etc. On the other hand, the MPC can be used as the basic units for constructing the first stage of the two-stage quasistationary high current plasma accelerator (QHPA) (Morozov, 1990). Namely, a combination of several MPC can be used to produce fully ionized plasma at the entrance to the acceleration channel of QHPA. Among the different fields of QHPA applications we are mentioning here only its using as the plasma injector in some fusion devices (Ananin *et al*., 2002).

The aim of this work is to enlarge the knowledge about the MPC operation and to improve methods of controlling its plasma parameters. The emphasis is on the investigation of a quasistationary phase of compression plasma flows and development of the appropriate methods for measuring of their electrical and thermodynamic parameters.

2. BASIC THEORY OF QUASISTATIONARY PLASMA ACCELERATORS

Quasistationary plasma accelerators are sources of quasistationary compression plasma flows in which the life time of the compression stable state is much longer (~100-1000 μs) than the flight time of the plasma in the acceleration channel of the accelerator (~1 μs) (Morozov, 1975). During a quasistationary phase the plasma flow parameters are slowly changing in time within certain volume (space). It is a consequence of an ion-drift acceleration of magnetized plasma realised using especially shaped accelerating channel (Morozov, 1990).

Elementary analysis of plasma flow (Morozov, 1990) based on the thin-tube aproximation showed that the accelerating channel has to have Laval nozzle profile. On the bases of equation of continuity, Bernoulli equation and magnetic flux conservation laws in standard notation:

$$df\rho v = const \tag{1}$$

$$\frac{v^2}{2} + i(\rho) + \frac{B^2}{\mu_0 \rho} = const \tag{2}$$

$$\frac{B}{\rho d} = const \tag{3}$$

the basic plasma parameters can be determineded. Here $i(\rho) = \int dp / \rho$ is enthalpy, f is the width of the tube and d is its average radius. Two extreme approximations can be used as follows.

In the acceleration regime, neglecting the enthalpy, maximal plasma velocity at the exit of the acceleration channel is $v_m = \sqrt{2} v_{A0}$. Here $v_{A0} = B_0 / \sqrt{\mu_0 \rho_0}$ is Alfven velocity at the entrance to the channel. With discharge current 100 kA (magnetic field 0.4 T at 5 cm distance from the electrode) and plasma density 10^{16} cm^{-3} for a hydrogen plasma, calculated plasma velocity at the exit of the channel is approximately 100 km/s.

As a result of this analyses one can find the dependences of maximal plasma velocity and voltage (between the electrodes) on discharge current and mass flow rate: $v_m \sim I^2 / \dot{m}$ and $U \sim I^3 / \dot{m}$, respectively. The dependences prove that the acceleration processes are predominantly determined by discharge current and mass flow rate. A deviation of the experimentally obtained dependencies from the above mentioned ones is the measure of the acceleration efficiency of the accelerators system as a whole.

In the compression regime (enthalpy included) degree of plasma compression in acceleration channel is:

$$\frac{\rho_{\max}}{\rho_0} = \left[(\gamma - 1) \frac{v_{A0}^2}{v_{S0}^2} \right]^{\frac{1}{\gamma - 1}} \tag{4}$$

and maximal temperature:

$$T_{\max} = \frac{\gamma - 1}{\gamma} \cdot \frac{M}{k} \cdot v_{A0}^2 \tag{5}$$

Here ρ_0 is electron density and $v_{S0} = \sqrt{\gamma \cdot p_0 / \rho_0}$ sound velocity at the entrance to the acceleration channel. With Alfven velocity 100 km/s and sound velocity 10 km/s, for adiabatic compression of hydrogen plasma ($\gamma=5/3$), maximal degree of compression is 550 and temperature 50 eV for these conditions.

From the above given analyses it follows that the increase of main plasma flow parameters (electron density and temperature and plasma flow velocity) can be achieved by an increase of the discharge current. However, large increase of the discharge current causes intense potential jump near anode and its heavy erosion. This cannot be avoided by the system with continual solid anode due to current slippage on its surface. Similar effects are seen in pulsed systems (plasma focus devices). However, these problems can be solved enabling an ion current transport in the accelerating system. The ion current transport has to be through the transparent anode and therefore the anode is made of rods (Morozov, 1990). For the same reasons, the cathode has to be made of rods. However, in this work it is only specially shaped.

A distinctive characheristic of compression flow is the "freezing" of magnetic field into plasma. In this type of plasma flows the existence of current loops (vortices) is detected. Namely, the presence of "swept-away" current into the compression plasma flows has been earlier noticed. The existence of the "swept-away" current is due to magnetic flux conservation (the magnetic field is frozen in plasma). It has been showed recently, that during an action of compression plasma flow on a sample surface current loops (vortices) can arise (Ananin *et al*., 1998).

3. EXPERIMENTAL SET-UP

The Magnetoplasma compressor of compact geometry (MPC-CG) used in this experiment was described elsewhere (Astashinskii *et al*., 1989; Astashinskii *et al*., 1991; Doichinovich *et al*., 2001), therefore only a few details are given here for the sake of completeness.

The electrode system of MPC (Fig. 1) consists of the conically shaped copper central electrode (cathode) with radius 3 and 0.6 cm, 5 cm in length, with divertor on the top. Cylindrical outer electrode (anode) is made of 8 copper rods (0.8 cm in diameter and 14 cm in length), symmetrically positioned along the circle of 5 cm in diameter. Conically shaped cathode of MPC defines the profile of the acceleration channel.

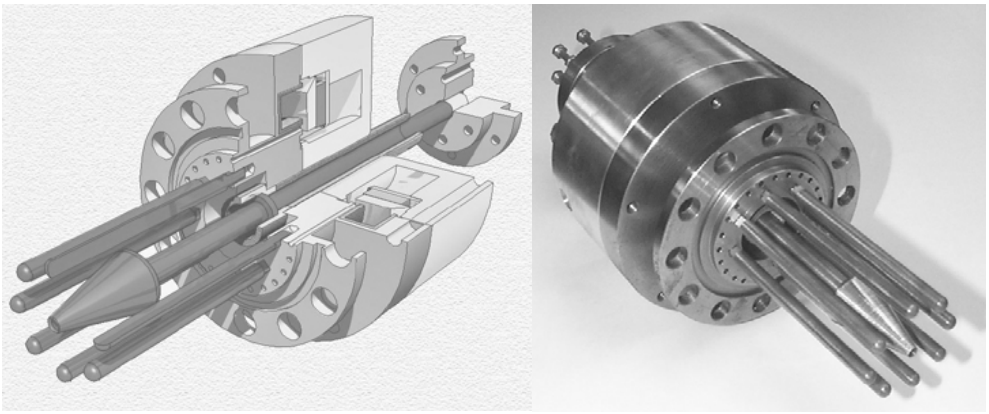

Fig. 1: Magnetoplasma compressor of compact geometry (MPC-CG).

The ions can be introduced into the acceleration channel through anode made of rods from the region between anodes rods and vacuum chamber being produced by "swept-away" currents. Namely, the gas around the anode is playing the role of virtual electrode. The self-magnetic field shielding of the anode rods (transparent anode) diminishes the level of the erosion. Anode rods are connected with the carrier, which enables MPC connection to the vacuum chamber.

A specially shaped insulator is positioned between anode rods carrier and the cathode to avoid the discharge breakdown on the surface of the insulator. It diminishes the level of impurities in plasma (Astashinskii *et al*., 1989). The insulator quality and its shape together with sufficient distance between carrier and the cathode enabled necessary

stability of the ionization zone, i.e., its shifting towards the insulator is avoided (Ananin *et al*., 1990).

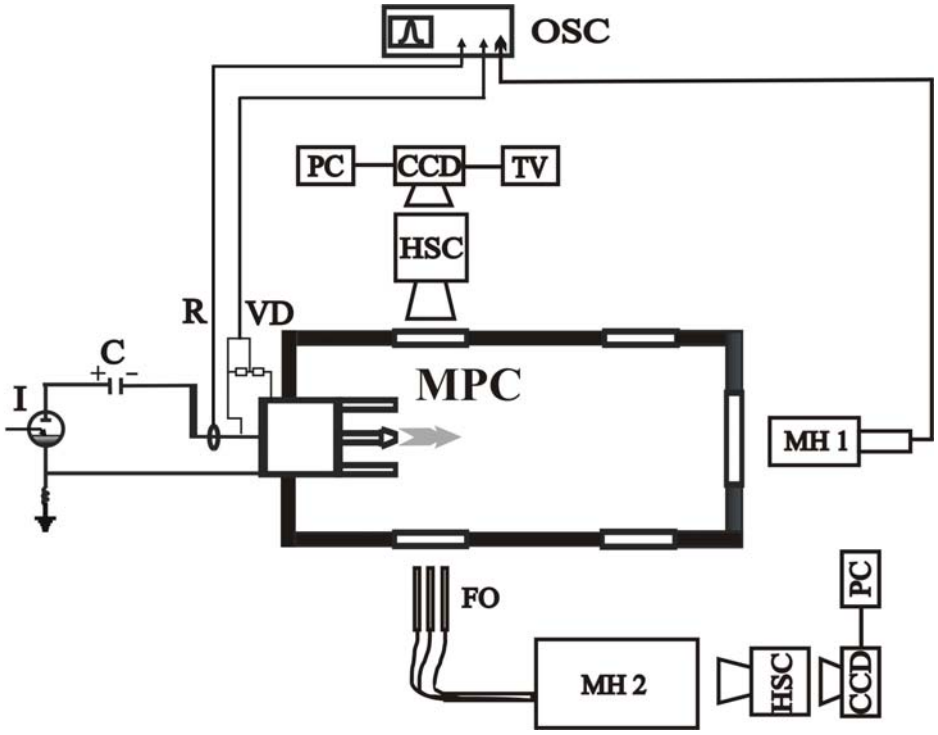

Fig. 2: Experimental set-up: C - capacitor, I - ignitron, OSC - oscilloscope for signals registration from Rogovski coil (R), voltage divider (VD) and McPherson spectrometer (MH1), HSC - high speed camera, FO - fiber optics, MH2 - Jobin Yvon spectrometer.

Stability of the compression plasma flow is achieved by the azimutal discharge simetry and homogeneous discharge current distribution through the electrodes surfaces. The discharge simetrisation is achieved by the special sectional formation of the condenser bank energy supply, appropriate connection design and continual working gas introduction through transparent anode.

In order to obtain as pure as possible plasma flow by MPC the ion separation per *M/q* (Morozov, 1969) the cathode top is shaped as a divertor. Due to Lorenz force heavier impurity ions stay close to electrode, e.g. go into divertor. If particular ion leaves the cathode, the high pressure zone ($\sim 10^4$ Pa) of the plasma flow pushes it back into divertor.

The discharge device of MPC is situated in a 30 x 30 x 150 cm vacuum chamber. Two-stage mechanical vacuum pump is used to evacuate the MPC vacuum chamber below 1 Pa; and then the chamber is filled with different working gas at given pressures. The MPC can operate with different working gasses and their mixtures as Ar, H_2, N_2, Ar + 3% H_2, at various pressures in two following modes: the working gas can be introduced using an electromagnetic pulse valve system witch allows mass rate in the range from 3-12 g/s; and in the regime of residual gas at different pressures from 10 to 10000 Pa. All measurements described here have been made with MPC operating in the residual gas

regime. The electrode system is connected through an ignitron (I) with 800 μF capacitor banks (C) (Fig. 2). Discharge current and the voltage between the MPC electrodes were measured using the Rogovski coil (R) and the voltage RC-divider (VD), respectively. The signals were simultaneously recorded by two-channel Tektronix TDS3032 oscilloscope (OSC).

Time and space developments of compression plasma flows and plasma velocity were determined using the photographs obtained by IMACON 790 high speed camera (HSC) operating in frame and streak modes (Fig. 2). For synchronization a sensitive photocell trigger unit was used.

Imaging technique performs digitalization during recording. CCD video camera, coupled to Imacon's output screen, gives composite video output to be fed into the PC. Video board performs capturing in real time and storing digital information in memory. When the recording ends, image processing software enables choosing the maximum illuminated frame from the video recording. For very low light level recording (for optical spectra) the image intensifier can be mounted on the Imacon's exit screen. Then CCD is optically coupled to intensifier's output screen. The exposure of CCD is not critical since the persistence of the Imacon's output phosphor is 80 μs.

Plasma velocity and shock front velocity were determined from streak records, using parallelly positioned slit with compression plasma flow axis in front of IMACON camera. The calibration of high-speed camera was effected using "Pulse generator" Hadland Photonics as a calibrator, within frequency range from 1 kHz to 100 MHz.

The electron density and temperature time dependences are obtained from end-on and side-on observations (Fig. 2). The profiles of spectral lines were obtained observing by shot by shot technique from the front side of MPC and averaging over several shots using McPherson 218 spectrometer (MH1, with Ar+3%H_2 as a working gas) and by side on observation using IMACON 790 high speed camera equipped with intensifier and CCD camera for line profile registration using Jobin Yvon HR 320S spectrometer (MH2, with H_2 as a working gas).

Time and spatially resolved spectroscopy measurements of hydrogen Balmer alpha line radiation from MPC plasma have been made using a HR320S spectrometer - IMACON 790 high speed camera system. Plasma was observed through a set of 10 fibers (FO) distributed along z axis starting from the outlet of the cathode with 7 mm separation up to 6.3 cm distance. All optical fibers were mounted in a certain order onto the entrance slit of the monochromator. It offers the possibility to obtain a set of line profiles in one shot at different positions from the cathode and at different times.

4. ELECTRICAL AND ENERGY DISCHARGE PARAMETERS

Analyzing the obtained current and voltage signals the electrical and energy discharge parameters were determined. Using such parameters it was possible to conclude whether or not the compression plasma flow was organized properly. Typical oscilloscope current and voltage traces for MPC operating in Ar + 3% H_2 are given in Fig. 3 (a).

The obtained current maximum was up to 100 kA, duration up to 150 μs (current half period ~70 μs), inductivity 0.5-0.7 μH and resistance 30-40 mΩ. The existence of phase shift between the current and voltage proved the absence of the discharge breakdown along the insulator surface (Astashinskii *et al*., 1989).

Using the current and voltage traces from Fig. 3 (a) the discharge volt-ampere characteristics (Fig. 3 (b)), as well as the change of the instantaneous input discharge power $P(t) = I(t) \cdot U(t)$ (Fig. 3 (c)) and energy $W(t) = \int I(t) \cdot U(t) dt$ (Fig. 3(d)) are obtained. Volt-ampere curves are nonlinear in the time interval from 20 to 50 μs when the plasma flow is quasistationary stable which can be regarded as the verification of the effectiveness of the MPC operation.

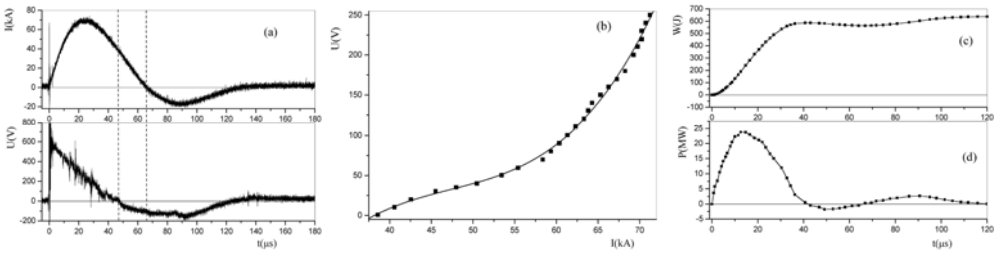

Fig. 3: Current and voltage oscilloscope traces (a), discharge volt-ampere characteristic (b), instantaneous power (c) and energy (d) time dependences.

Linear volt-ampere characteristics were obtained in the case of classical plasma accelerators with continual electrodes (Kovrov and Shubin, 1974), as well as in the case of atmospheric pressure discharges (Astashinskii *et al.*, 1991). There is no phase shift between current and voltage if the discharge breakdown is going on the isolator surface. Therefore volt-ampere characteristics are linear. From Fig. 3 (d) one can conclude that the energy transfer from capacitor bank to the discharge is terminated at the end of the first current half-period (~60 μs).

Analyzing volt-ampere characteristics of discharge in Ar, N_2 and H_2 (Fig. 4) one can conclude that most effective energy transfer from supply to plasma is in hydrogen as a working gas (largest volt-ampere characteristics slope).

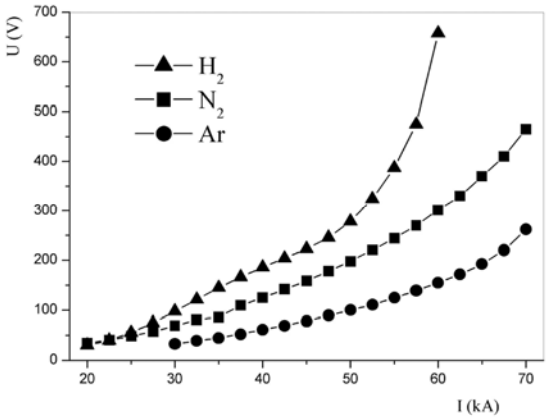

Fig. 4: Discharge volt-ampere characteristic in Ar, N_2 and H_2.

5. COMPRESSION PLASMA FLOW IN TIME EVOLUTION

Using IMACON 790 high speed camera operating in frame and streak mode, the evolution in time of breakdown, shock wave formation, compression plasma flow creation and after glow discharge were registered in Ar, N_2 and H_2 at 10-3000 Pa pressures, and 2.5-4.1 kV voltages.

Although MPC discharge development depends on the initial conditions, first of all working gas and its pressure, as well as on energy supply voltages, a general picture of the dynamics of the compression plasma flow formation can be obtained on the bases of high speed camera images (Fig. 5). Discharge development can be divided in four phases: (i) discharge breakdown and plasma accelerating along the cathode conical part; (ii) radial plasma compression and relaxation of accompanied plasma flow oscillations; (iii) quasistationary stable state of compression plasma flow; (iv) decay of compression plasma flow followed by after glow effects.

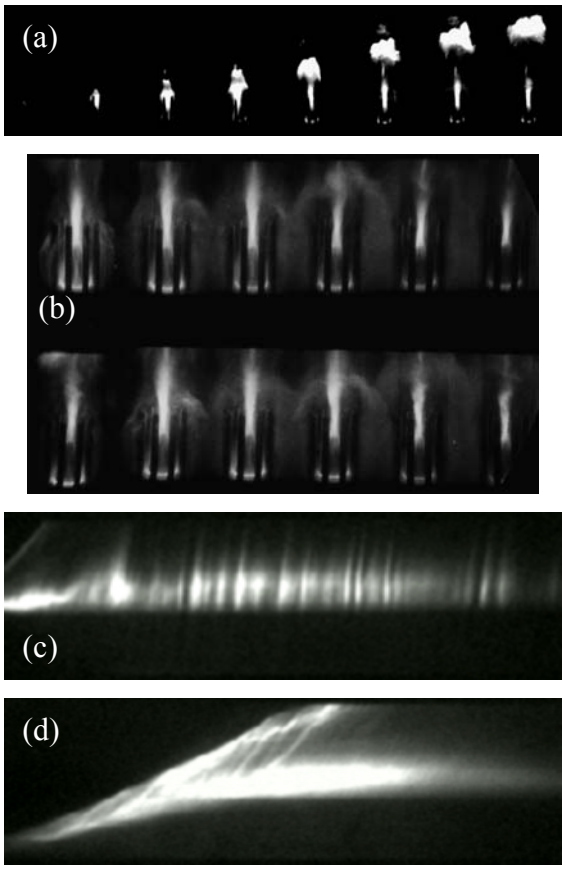

Fig. 5: MPC discharge development in argon obtained by IMACON 790 high speed camera operating in framing mode with time intervals of 4 μs (a) and 2 μs (b) and exposure time 400 ns; and streak mode with 1 μs/mm at 100 Pa (c) and 3000 Pa (d) pressures.

The first phase starts after the triggering pulse switching on ignitron, resulting with discharge breakdown in the inter electrodes region of MPC lasting till the plasma gets out from that region. The breakdown starts at the top of the cathode (maximal distance from the anode rods) or from the widest conical cathode part (narrowest cross section of the accelerating channel, i.e. minimal distance from anode rods) depending on the working gas pressure. During this phase discharge current increases and therefore the magnetic field increases, too. At the real beginning of the discharge, the electric field is established in the whole volume of the accelerating channel. However, the increasing magnetic field, carrying practically the whole energy, is established only at the entrance to the acceleration channel. In the MPC inter electrode region the plasma is accelerated due to the Ampere force F_{Az} as the result of the radial component of plasma current I_r interaction with azimuth magnetic field B_φ: $\vec{f} = \vec{j} \times \vec{B}$ (Fig. 6).

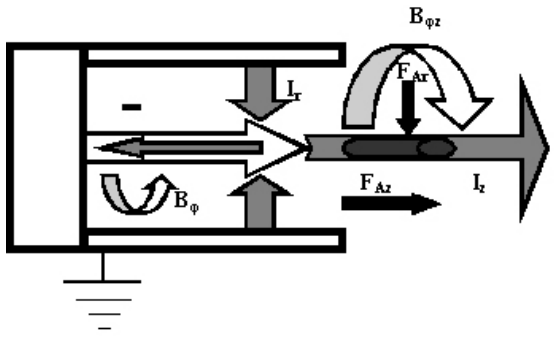

Fig. 6: Scheme of MPC principle.

It is found that plasma during this phase reaches the end of the electrodes after about 5-10 μs from the beginning of discharge.

The second phase usually starts with strong radial plasma compression at the top of the cathode lasting up to plasma oscillations relaxation within compression flow. This is the transition phase to a quasistationary (stable) phase. At the beginning of the phase the first plasma front is formed initiating a shock wave. At the same time axis-simetrically in the accelerating system, at the outlet of MPC, the compression plasma flow is created (Fig. 5). The compression plasma flows are formed about 15-20 μs after the beginning of the discharge current. The only exception is in hydrogen when this process is going on during ~10 μs. Plasma flow is compressed due to interaction between the longitudinal component of current swept-away I_z from discharge device, and intrinsic azimuth magnetic field $B_{\varphi z}$ (Fig. 6), as well as, due to the dynamic pressure of plasma flow converging to the system axis (the inertial compression). The presence of the "swept-away" current in the plasma flow is caused by the magnetic field frozen in plasma.

The energy from condenser bank supply is transferred to the plasma through magnetic field. The plasma is accelerating and therefore its kinetic energy is increasing. Due to plasma compression its enthalpy is increasing. After plasma leaving the compression zone, its total energy again is transferred in plasma kinetic energy.

During this second phase an ionization zone is formed in the region of accelerating channel having minimal cross section (Fig. 5). Ions produced by "swept-away" current in the external region behind the anode made of rods, come to the accelerating channel. Within 15-30 μs the radial oscillations of compression plasma flow occur.

The first plasma front after coming to the top of cathode, is leaving inter-electrodes part of the MPC being followed by the compression plasma flow formed at the cathode top. The front is occupying the deceleration zone of compression plasma flow due to its interaction with working gas.

The third quasistationary phase is starting after termination of the above described transitional processes when a stable compression plasma flow is created. Shape and duration of compression plasma flow depend on the working gas and its pressure, as well as on input energy. For instance, durations of compression plasma flow in Ar and N_2 are shorter at high pressures (~30 μs) than at low pressures (~40 μs). However, in hydrogen the stable compression plasma flow exists about 50 μs. During this phase plasma parameters are changing slowly and conditions for local thermodynamic equilibrium (LTR) are fulfilled.

It this experiment it has been found that the compression plasma flow length is the function of the working gas, the pressure and discharge current. Generally, the length is increasing with pressure lowering and maximum discharge current increasing. It is especially expressed in argon as a working gas and, also, in hydrogen but at lower pressure (Fig. 7). Diameters of compression plasma flows are 0.5-1.5 cm in the zone of maximal compression. It was found that they decrease with pressure decreasing and discharge current increasing.

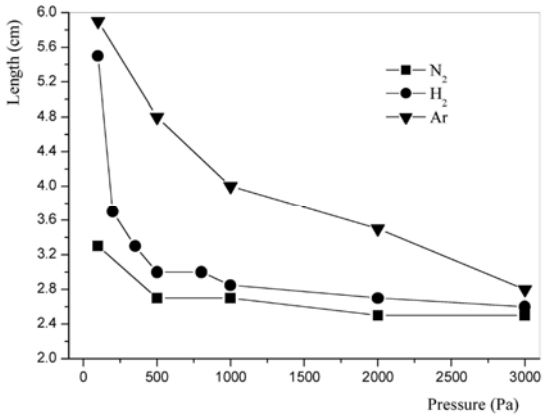

Fig. 7: Length of compression plasma flow for different working gases as the functions of pressure.

Compression plasma flow velocities are measured using photographs obtained by high speed camera operating in streak mode similar to one presented in Fig. 5. In this Figure a discrete microstructure of compression plasma flow (light and dark regions) is observed. These structures are occurring with 5-10 MHz frequencies. From the slopes of the structures compression plasma flow velocities are determined and given in Fig. 8 for

different working gases as the functions of pressures. From Fig. 8 one can conclude that plasma flow velocities in argon and nitrogen are decreasing with pressure increasing.

However, in hydrogen the maximum value of plasma flow velocity is observed at 1000 Pa pressure. For pressures lower than 1000 Pa the plasma flow velocity is decreasing with pressure decreasing. This can be explained by the enhanced erosion of the cathode at pressure lower than 1000 Pa. It is a consequence of the impurities present in the plasma flow (mass of working gas is increased). This effect is not found in the case of nitrogen and argon as working gas, although from Fig. 8 one can conclude that for 100 Pa pressure in all cases plasma flow velocities are almost the same.

It is of interest to note once again that maximal plasma flow velocity values are obtained for hydrogen. This, together with non-linear volt-ampere characheristics shape, proves that the hydrogen is the most favorable working gas in MPC, regarding the energy transfer effectiveness from the condenser bank supply to plasma.

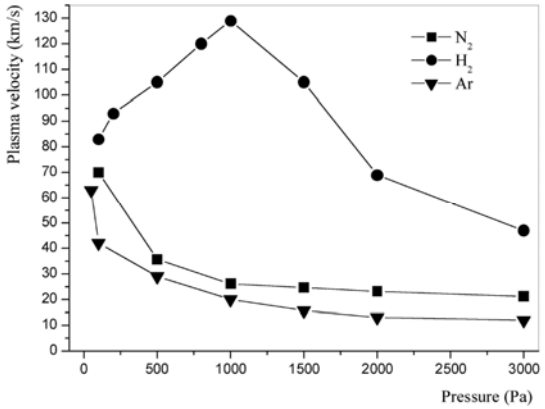

Fig. 8: Plasma flow velocity for different working gases as the functions of pressure (6.4 kJ supply energy).

MPC-CG is a quasistationary plasma source because life time of the created compression flow is much longer than characteristic flight time of plasma in the accelerating channel. For the average plasma velocity of 50 km/s (5 cm/μs) and accelerating channel ~5 cm long, flight time is ~ 1 μs. The stable compression plasma flow state is terminated 70-80 μs after the discharge beginning. It is in good accordance with current pulse duration.

The fourth phase of the MPC operation is the compression plasma flow decay. Its beginning and duration depend on the initial conditions determined by the characheristics of condenser bank energy supply. If the input energy can be continually supplied quasistationary phase can be unlimited in time and the decay phase can be unlimitedly postponed.

In that case MPC will operate as stationary plasma source. Namely, the continual ionization processes are taking part in working gas introduced in interelectrode region. The ionized gas (plasma) is steadily accelerated and permanently compressed.

In this experiment the duration of MPC discharge is approximately 140 μs for energy supply of 5-10 kJ. However, plasma current loops owing to the magnetic field

confined in plasma can exist longer in chamber disappearing slowly at the chamber walls. The so-called swept away currents have sufficient energy to excite the atoms and ions of working gas. Therefore, the radiation from the working gas lasts longer then the discharge in the accelerator (Doichinovich *et al*., 2001).

The presence of cathode erosion (Fig. 9 (a)) as well as anode protection from the erosion can be regarded as the proof of the ion current transport occurring. The cathode erosion is a consequence of cathode potential drop and current slippage along the cathode surface.

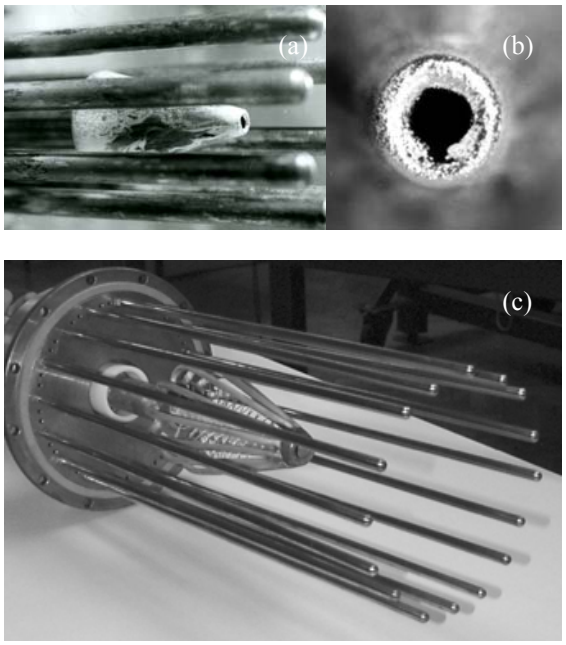

Fig. 9: Erosion of MPC cathode: (a) side on image; (b) the top of the cathode image; (c) MPC with transparent electrodes (self shielded by magnetic field).

The cathode erosion is especially intensive in MPC working in argon at low pressure (~100 Pa). Also, the material deposition originating from the cathode is present at the divertor top (Fig. 9 (b)).

In order to avoid cathode erosion it has been specially designed and constructed similarly to the one used in accelerating channel of two stage quasi-stationary plasma accelerator (Ananin *et al*., 1990; Morozov, 1990; Kuraica *et al.*, 2002) (Fig. 9 (c)).

6. PLASMA FLOW PARAMETERS

Plasma flow electron density and temperature are measured using spectroscopy methods. Plasma reproducibility was within ±10% as measured from intensity of continuum

radiation. The estimated experimental errors of plasma electron density and temperature measurements are within ±10% and ±15%, respectively. Electron density is determined using Stark profiles of H_α and H_β spectral lines analyses (Fig. 10). The profiles were obtained using shot-by shot technique, observing from the front side of MPC and averaged over several shots when operating in Ar + 3% H_2 working gas mixture (Fig. 2). The electron density time dependences are obtained from the comparison of the measured Stark widths with theoretical results of Gigosos and Cardenoso (1996). They are presented in Fig. 11 (a).

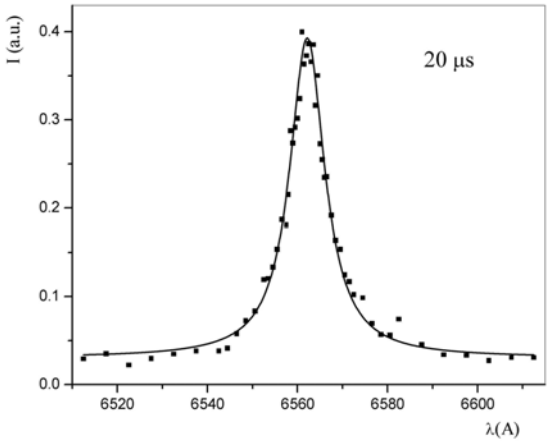

Fig. 10: Line profile of H_α as obtained by end-on observation in Ar + 3% H_2 mixture (n_e = $8 \cdot 10^{16}$ cm^{-3} and T_e = 13 200 K).

Compression plasma flow parameters predominantly depend on discharge current. Electron density time dependence correlation with discharge current time evolution is determined by a dynamical coefficient n_e/I (Ananin *et al*., 1998) (Fig. 11).

The dinamical coefficient n_e/I is a measure of plasma flow stationarity. It is constant when and where the compression plasma flow is quasi-stationary stable. Namely, electron density "follows" the discharge current time evolution. In the beginning of plasma flow creation n_e/I is decreasing, since discharge current increases faster than the electron density. However, during the compression plasma flow decay this parameter increases as a consequence of faster discharge current decreasing (in comparison with compression plasma flow vanishing).

Physical processes within compression plasma flows depend on the discharge current time dependence. These processes can be studied by the investigation of spectral lines and continuum radiation, as well as by the study of discharge current time dependence. Time dependences of several hydrogen spectral lines obtained in Ar + 3% H_2 gas mixture are given in Fig. 12.

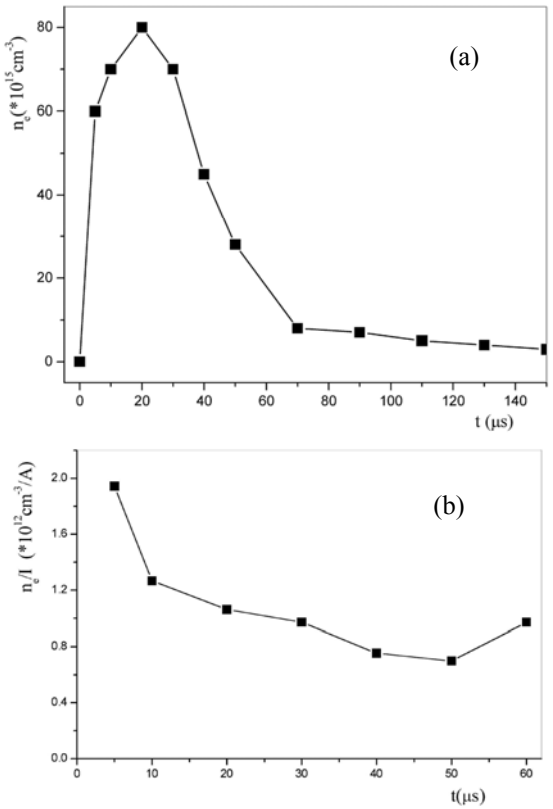

Fig. 11: The electron density (a) and dynamical coefficient n_e/I (b) time dependences.

From Fig. 12 one can conclude that the intensities of H_α, H_β and H_γ have reached their maximal values at different instants. It is found that H_α maximum is the latest in comparison with other two lines maxima (H_β and H_γ). The maxima of all investigated lines are very wide (with constant intensity for about 20 μs). The intensities of H_α and H_β spectral lines last 3 to 4 times longer than the current signal (signal from Rogovski coil). That effect of the afterglow radiation existence was observed, also, for the neutral argon line intensities (ArI 696.5 nm).

The continuum and ion argon line intensities time dependences on compression plasma flow of MPC operating in Ar + 3% H_2 gas mixture are also analyzed. Continuum radiation and the Ar II 480.6 nm spectral line intensities (Fig. 12) are following the discharge current time dependence, reaching maximal values at the same time (~25 μs), although intensities of singly charged argon ion lines last longer (up to the end of discharge current second half period ~130 μs) than the continuum radiation (up to the end of the first half period ~80 μs). It is obvious that the argon ions are emitted from the most compressed region of the plasma flow. When the discharge is terminated the compressed plasma flow is disappearing, and the argon singly charged ions are neutralized by recombination.

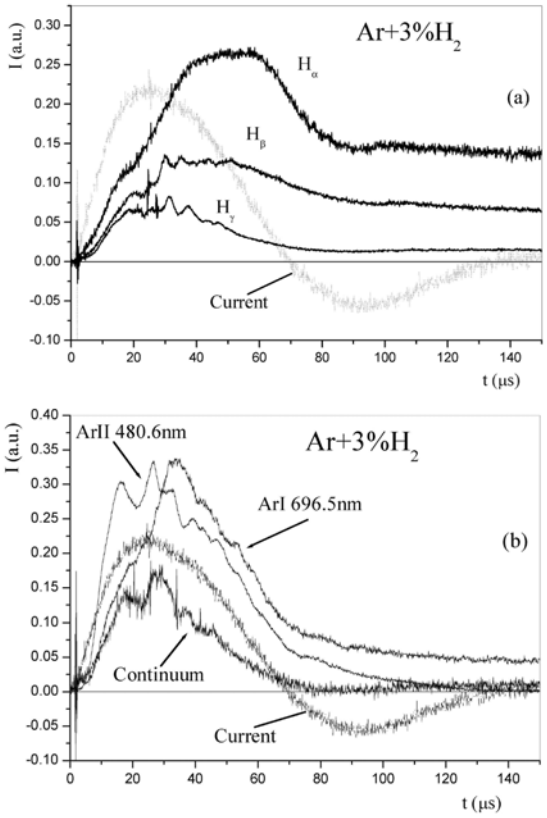

Fig. 12: Intensities of: a) H_α, H_β and H_γ; b) ArI 696.5 nm, Ar II 480.6 nm spectral lines versus time compared with continuum radiation intensity and discharge current time evolutions.

The intensity maxima of all spectral lines are appearing in the time interval (20-60) μs from the beginning of discharge, i.e. in the period of maximal compression of the plasma flow. In that period the plasma flow is in quasistationary stable state, which is verified by Fig. 6. The compression plasma flow starts disappearing 70 μs after beginning of the discharge. The swept away currents have enough energy to excite hydrogen and argon atoms and due to that, the radiation is observed several hundreds microseconds after the discharge termination (Doichinovich *et al*., 2001).

The axial and temporal electron density distributions of the compression plasma flow are obtained from the Stark halfwidth of Balmer alpha line profiles comparison with theoretically calculated ones (Gigosos and Cardenoso, 1996). Measurements have been made in pure hydrogen at 1000 Pa pressure from side on observation. The experimental setup used is given in Fig. 3. Spectral line intensities registration was performed using high speed camera operating in framing mode ($1 \cdot 10^5$ frame/s) and thereby from the analyses of these profiles the electron density axial distribution in time was enabled. One hundred of H_α profiles were obtained per one MPC shot using this method.

Temporal and spatial electron density distribution of MPC plasma determined using Stark profiles of H_α spectral lines are given in Fig. 13. Electron density has its maximum at 20 μs and is approximately constant ~$(3\text{-}4)\cdot10^{17}cm^{-3}$ within the 0.5-4 cm region along the z axis. For distances greater than 4 cm an appreciable electron density is noticed only at 10 μs record, which can be explained by the action of shock wave on the ionization of working gas. Contrary to this, after 10 μs electron density suddenly decreases for all positions larger than 4 cm, i.e. out of compression plasma flow region.

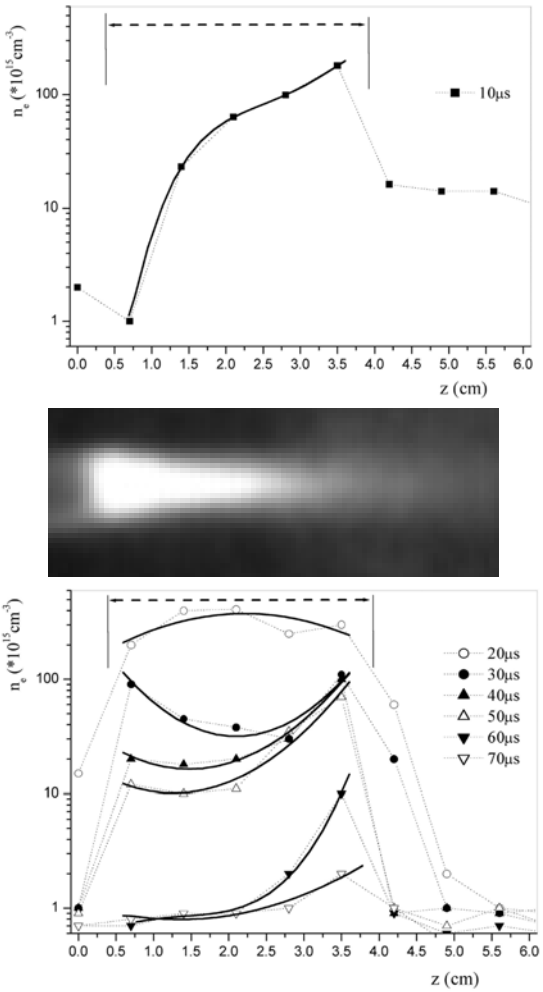

Fig. 13: The electron density time dependences from side-on observation in H_2 with one high speed camera frame.

The axial and temporal distributions of Balmer alpha line intensity are given in Fig. 14. An increase of line intensity during 20 μs rise time is found in every position along the MPC z axis. Maximum line intensity reached at 20 μs is constant from 0.5 to 4.5 cm from the top of the cathode, along the z axis. Balmer alpha line intensity then decreases versus

time in every position. The maximum of line intensity is observed within the 1.5-2 cm region in time interval of 30-70 μs. Further than 4.5 cm along z axis line intensity is very low for every time record.

By comparing the obtained Balmer alpha line intensity and the electron density axial distribution in time one can come the following conclusions: (i) both distributions have their maxima 20 μs after the discharge beginning, gradually decreasing later on; and (ii) a range of high values for both distributions is the same and is localized within 0.5-4 cm region along z axis.

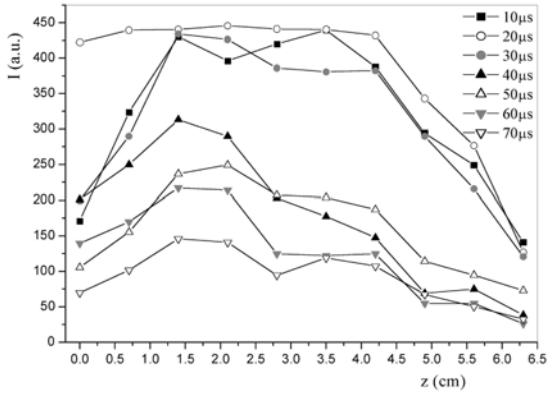

Fig. 14: The Balmer alpha line intensity time dependences from side-on observation in H_2.

All this can be regarded as the verification of stable quasistationary compression plasma flow existence, created by the MPC plasma accelerator.

In the paper of Astashinskii *et al.* (1992) it was reported that the electron density within accelerating channel is of the order of 10^{16} cm^{-3}. Here, we have found that electron density obtained by quasistationary plasma accelerator is a weak function of the working gas type and pressures and strongly dependent on the discharge current. Therefore, we have used this value in order to calculate the degree of compression and have obtained it to be approximately 20.

The electron temperature was measured in the MPC operating in Ar + 3% H_2 gas mixture using a method based on the relative intensity ratios of spectral lines originated from two successive ionization stages of argon, using Saha equation.

The experimental set-up used is given in Fig. 3. The measurement has been made using Ar I 696.5 nm and Ar II 480.6 nm argon line intensities by end on observation. The obtained electron temperature time dependence is given in Fig. 15. It was found that within quasi-stationary plasma flow region the average temperature is 13000 K, which is in good agreement with previous experiments (Ananin *et al*., 1990; Astashinskii *et al.*, 1992).

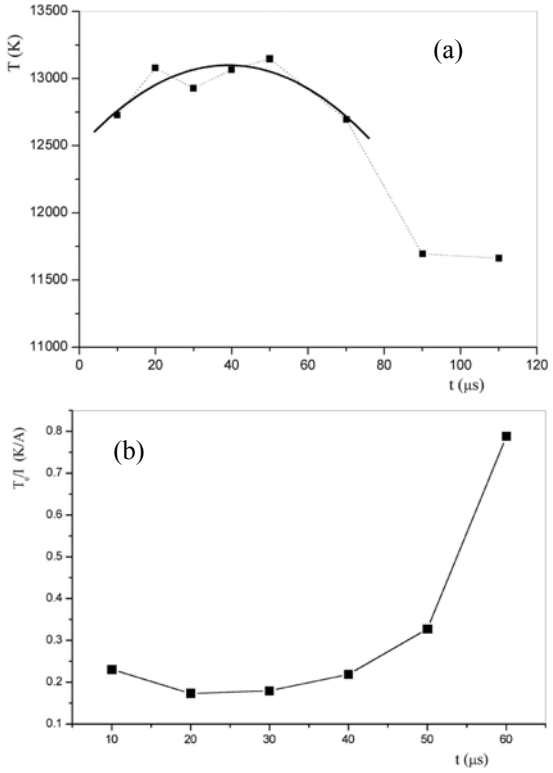

Fig. 15: The electron temperature (a) and dynamical coefficient T_e/I (b) time dependences.

Similarly to the definition of dinamical coefficient of electron density, it is of interest to do the same for electron temperature (T_e/I). It was calculated from the experimentally obtained values of temperature and discharge current and presented in Fig. 15. It was found that during the quasi-stationary phase this parameter is constant. However, during compression plasma flow decay this parameter increases which is in good accordance with conclusion drawn in the case of n_e/I dinamical coefficient behavior.

Using the equation for an ideal gas state it is possible to calculate gas kinetic pressure within compression plasma flow. For 1-2 eV temperature and 10^{17} cm^{-3} density, the pressure is of the order of 10^4 Pa.

Compression plasma flow current can be calculated from the balance between the gaskinetic plasma pressure and azimuth self-magnetic field pressure

$$\frac{B^2}{2\mu_0} = nk(T_e + T_i) \tag{6}$$

e.g. from Benet equation (with $T=T_e=T_i$)

$$\mu_0 I^2 = 16\pi^2 R^2 nkT \tag{7}$$

where R is the radius of compression flow.

In this experiment for $n_e \sim 2 \cdot 10^{23}$ m^{-3}, $T_e \sim 15000$ K, $R \sim 8 \cdot 10^{-3}$ m, and consequently plasma flow current is ~15 kA, which is 20% of the discharge current maximal value (~80 kA).

7. CONCLUSION

The advantages of magnetoplasma compressor of compact geometry, as compared to other types of accelerators, are high stability of the compression flows generated, controllability of their composition (different gases and their mixtures), size (up to 6 cm in length and 1 cm in diameter), and plasma parameters (up to $4 \cdot 10^{17}$ cm^{-3} and temperature up to 2-3 eV), as well as the discharge duration sufficient for practical applications (up to 70-80 μs). Besides, the operation in the ion current transfer mode with the minimization of the electrodes erosion represents the main advantage of the quasistationary plasma accelerators in comparison with the classical ones. Also, there is no limit in increasing their main parameters (plasma flow duration, flow velocity, temperature and plasma density) due to the discharge current cut off in the case of classical plasma accelerators. The "current crisis" can be avoided by the electrodes protection from the erosion as a result of the magnetic field self shielding. All limitations are connected with input energy of the accelerator. Therefore, MPC described here is a favorable one for constructing the first stage of two stage quasi-stationary plasma accelerator which can be used as possible plasma injector in fusion device and investigation of plasma wall interaction in fusion reactor.

References

Ananin, S.I., Astashinskii, V.M., Bakanovich, G.I., Kostyukevich, E.A., Kuzmitski, A.M., Man'kovskii, A.A., Min'ko, L.Ya., Morozov, A.I.: 1990, *Sov. J. Plasma Phys*., **16**, 102.

Ananin, S.I., Astashynski, V.M., Burakov, V.S., Kostyukevich, E.A., Kuzmitski, A.M., Tarasenko, N.V., Dojcinovic, I., Kuraica, M.M., Puric, J., Videnovic, I.R.: 2002, *29th EPS Conference on Plasma Phys. and Contr. Fusion*, Montreux 2002, Switzerland, **26B**, P-5.049.

Ananin, S.I., Astashinskii, V.M., Kostyukevich, E.A., Man'kovskii, A.A., Min'ko, L.Ya.: 1998, *Plasma Physics Reports*, **24**, 936.

Astashynski, V.M., Ananin, S.I., Askerko, V.V., Avramenko, V.B., Kostyukevich, E.A., Kuzmitski, A.M., Uglov, V.V., Anishchik, V.M., Astashynski, V.V., Kvasov, N.T., Danilyuk, A.L., Purić, J., Kuraica, M.M., Dojčinović, I., Videnović, I.R.: 2002, *16th ESCAMPIG*, Grenoble 2002a, France, **1**, 149.

Astashynski, V.M., Ananin, S.I., Askerko, V.V., Avramenko, V.B., Kostyukevich, E.A., Kuzmitski, A.M., Uglov, V.V., Anishchik, V.M., Astashynski, V.V., Kvasov, N.T., Danilyuk, A.L., Puric, J., Kuraica, M.M., Dojcinovic, I., Videnovic, I.R.: 2002b, *29th EPS Conference on Plasma Phys. and Contr. Fusion*, Montreux 2002, Switzerland, **26B**, P-2.027.

Astashinskii, V.M., Bakanovich, G.I., Kuzmitski, A.M., Min'ko, L.Ya.: 1992, *Journal of Engineering Physics and Termophysics*, **62,** 281.
Astashinskii, V.M., Bakanovich, G.I., Kostyukevich, E.A., Kuzmitski, A.M., Man'kovskii, A.A., Min'ko, L.Ya.: 1989, *J. Appl. Spectroscopy*, **50**, 887.
Astashinskii, V.M., Efremov, V.V., Kostyukevich, E.A.: 1991, *Sov. J. Plasma Phys.* (Engl. Transl.), **17**, 545.
Astashinskii, V.M., Min'ko, L.Ya., Man'kovskii, A.A.: 1991, *J. Appl. Spectroscopy*, **55,** 903.
Doichinovich, I.P., Gemishich, M.P., Obradovich, B.M., Kuraitsa, M.M., Astashinskii, V.M., Puric, Ya.: 2001, *J. Appl. Spectroscopy*, **68**, 629.
Gigosos, M.A., Cardenoso, V.: 1996, *Journal of Phys. B*, **29,** 4795.
Kovrov, P.E., Shubin, A.P.: 1974, *Physics and Application of Plasma Accelerators* (in Russian), Nauka i Tekhnika, Minsk, 1974, 78.
Kuraica, M.M., Astashynski, V.M., Dojčinović, I., Purić J.: 2002, *21st SPIG,* Soko Banja 2002, Serbia, 510.
Morozov, A.I.: 1969, *Nuclear Fusion Special Suppl.*, 111.
Morozov, A.I.: 1975, *Sov. J. Plasma Phys.* (Engl. Transl.), **1**, 95.
Morozov, A.I.: 1990, *Sov. J. Plasma Phys.* (Engl. Transl.), **16**, 69.